DESIGN OF CRYOGENIC(4.2K) X-BAND HEMT OSCILLATOR FOR JOSEPHSON VOLTAGE STANDARD

Moon-Que Lee, Sangwook Nam, Kyung-Whan Yeom*, and Kyu-Tae Kim**

School of Electrical Engineering, Seoul National University
Inst. of New Media and Comm., Seoul National Univ., Kwanakgu, Seoul, 151-742, Korea
lmk@inmac3.snu.ac.kr

Depart. of Radio Science and Comm. Eng., Chungnam National University

Korea Research Institute of Standards and Science

Abstract

A new oscillator configuration for Josephson voltage standard is proposed and designed by a novel method. An analytic design procedure is presented for general six configurations of oscillators with two loads. The power splitting relationship between two loads is derived with respect to the reactive(lossless) embedding element. A HEMT oscillator is designed in X-Band for the Josephson voltage standard and tested in room and cryogenic temperatures. There is a significant improvement of C/N ratio it is operated at cryogenic temperature(4.2K).

I. Introduction

When the microwave signal is injected into the Josephson junction, the output DC voltage produced by $V_n = nf/(2e/h)$ (n: integer), that is output DC voltage depends upon the applied source frequency and fundamental physical constant of $2e/h$. Based on this principle, the Josephson voltage standard system gives the order of the order of frequency measuring which can be measured with the highest precision among the physical quantities.

Recently, instead of an expensive superconducting microwave monolithic integrated circuits (SMMIC) based on series arrays of Josephson junctions, hybrid integration techniques are successfully used for establishing a Josephson series array[1]. Hybrid integration circuit(HIC) using the X-band microwave oscillator has advantages over SMMIC in views of cost, system complexity, energy consumption, and implementation. HIC oscillators of plastic package MESFET have been successfully applied to the Josephson voltage standard at cryogenic temperature of liquid helium, however the performance of HEMT oscillator has not been reported at this temperature to authors' review. In this paper, a HEMT oscillator of a new circuit topology is designed and tested for the application of the Josephson voltage standard of HIC type.

II. General Six Topologies of Oscillators with Two Loads

In many applications including Josephson voltage standard, oscillators have a coupling load in addition to the output load. In the stable oscillation system, this coupling load is used as a locking port for stabilizing the oscillation frequency. Couplers, power splitters or lumped passive elements are used for a coupling port. However these additional elements increase the complexity and size of circuit. To reduce the circuit size and complexity, it is required a new oscillator configuration which has a direct coupling load in addition to the output load.

In this paper, we present new six topologies of microwave oscillators shown in Fig. 1. The proposed configurations have two loads, one is for output port and the other is for coupling port.

III. Oscillator Design using Substitution Theory

An oscillator is composed of an active device and external feedback elements. The external feedback elements are usually determined for the active device to deliver maximum output power to the load. The feedback elements are calculated from the nonlinear or linear parameters of active device. So the characterization of the active device is required to maximize the output power.

0-7803-4471-5/98/$10.00 (c) 1998 IEEE

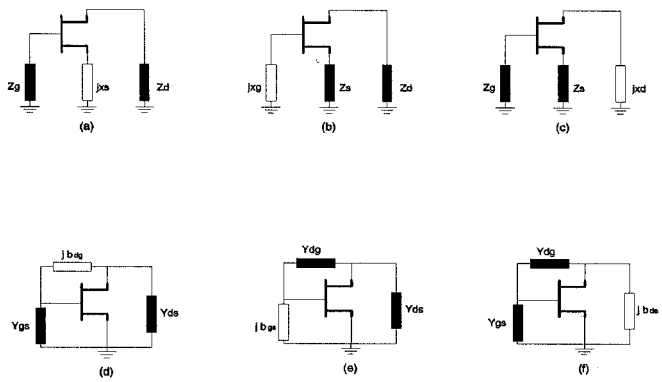

Fig. 1. Proposed six configurations of oscillators with a direct coupling load.

To analyze the active device, substitution theory for the embedding network is applied as shown in Fig. 2 [2]. In Fig. 2, embedding feedback elements are represented as the terminal voltages and currents. To optimize the output power of oscillator we have only to find out the input incident power level(P_{in}) and load(Γ_l) of Fig. 3.

For the ceramic package HEMT(FHX35LG), the results of substitution are shown in Fig. 4. The object of substitution is to obtain the terminal voltages and currents (V_1, I_1, V_2, and I_2) which give the maximum output power.

From Fig. 4-(a), the input power level can be selected at $P_{in} = 7$ dBm which is slightly below maximum DC-RF efficiency point. To find out the optimum load(Zopt) of Fig. 2, the load-pull is carried out, and the result is shown in Fig. 4-(b). The optimum load corresponding to maximum output power from Fig. 4-(b) is

$$Z_{opt} = 36.0241 + j3.6893 \quad . \qquad (1)$$

If RF terminal voltages and currents are obtained by using above approach, it is possible to determine the values of all elements of the generalized six basic oscillator configurations of Fig. 1.

Since the proposed configurations of oscillators have 5 variables(one lossless element and two loads), but the only four independent equations can be obtained from real and imaginary parts of network parameters. Therefore the embedding network elements can not be determined uniquely. The values of elements have under-determined solutions, and their solutions result in that the total power produced by active device is splitted into output load and coupling load with respect to the lossless element. The derived values of embedding feedback elements of six general configurations are given in Table 1 and 2.

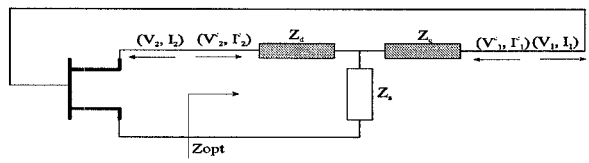

Fig. 2. Oscillator configuration with T-shape embedding elements.

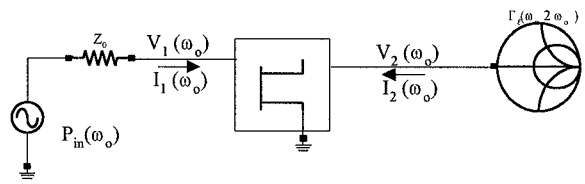

Fig. 3. Load-pull Method using substitution of embedding elements for the analysis of RF-operating point of oscillator.

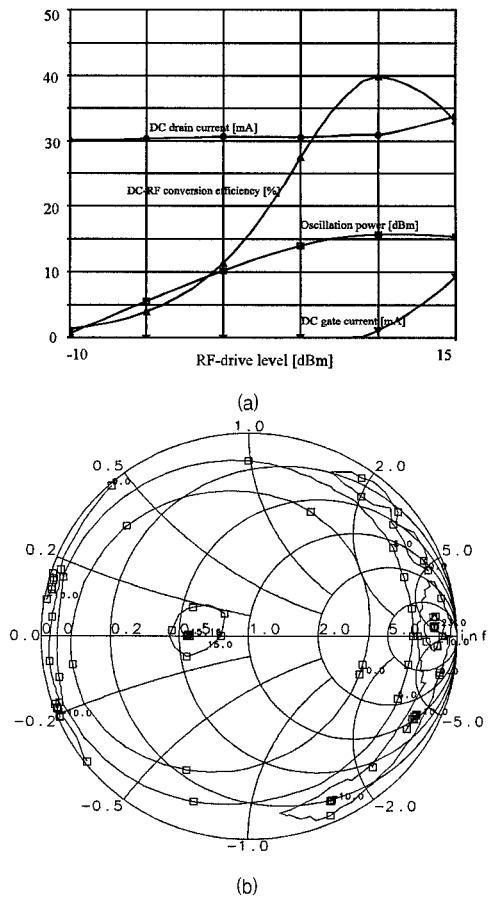

Fig. 4. (a) Sweep of RF-drive level $P_{in}(\omega_o)$ for determination of the optimum RF-drive level (FHX35LG HEMT, $Z_{opt} = 36.0241 + j3.6893$), (b) Results of load-pull of Fig. 6 (Pin=7dBm)

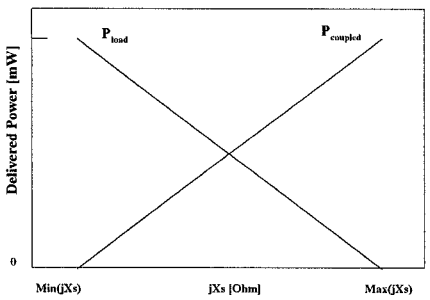

Fig. 5. Power splitting relationship versus the lossless feedback element.

If the value of lossless elements is selected within the specific oscillation range(for example, between min(jXs) and max(jXs) for case (a) in Fig. 1), the power splitting relationship between load and coupling load is depicted as Fig. 5. It is noted that the limit value of the lossless such as min(jXs) or max(jXs) coincides with the conventional oscillator with one load. That is, the conventional configurations are the specific cases of the proposed configurations, so the proposed configurations are extensions of conventional general six oscillators[3]-[5].

IV. Experimental Results

X-band HEMT(FHX35LG) oscillator with a coupling load is designed by above design approach at room temperature, and tested at temperature of liquid helium. Nonlinear model(EEHEMT) of the HEMT is used to optimize the output power by using substitution theory. For the oscillator configuration of case (a) in Table 1, the oscillator have following oscillation range.

$$j159 < jx_s < j2439 \qquad (2)$$

If we select j387 as the source reactance, the power relationship between load and coupling port has about 10 dB difference. Circuit pattern are realized in microstrip type except for the CPW transition between load and Josephson array. Glass-fiber reinforce teflon substrate(Chuko) of 654 um with 17 um copper layers is used. Ceramic package HEMT is used for the design. It has been reported that its performance such as output power and phase noise is superior to MESFET at 110K except current collapse[6]. The circuit layout pattern and its description are shown in Fig. 6. To avoid the current collapse, drain bias is selected slightly higher than maximum tansconductance drain voltage. The output powers of oscillator are shown in Fig. 7 and Fig. 8. Power difference of about 7dB between output load and coupling load is obtained at room temperature. C/N ratio of -70 dBc/Hz @50kHz is measured by spectrum analyzer(HP-8566B) at roon temperature. This C/N ratio @50kHz is significantly reduced by about 20dB at cryogenic temperature shown in Fig. 9. Output power at low temperature has also the higher value by 3.5dB. The short term stability is improved from 10^{-4} at room temperature to 10^{-6} at low temperature.

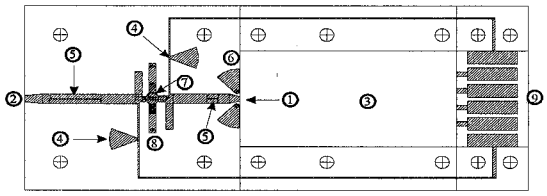

Fig. 6. Circuit layout :(70*30 mm^2)
①: load, ②: coupling load, ③: area of Josephson series array, ④: bias pattern, ⑤: DC blocking, ⑥: microstrip to CPW transition ⑦: HEMT(FHX35LG), ⑧: source impedance, ⑨: DC pad

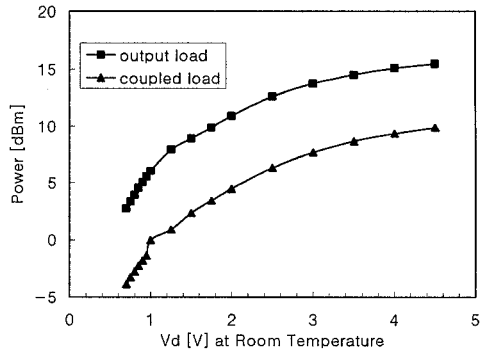

Fig. 7. Load and coupling powers of the implemented HEMT oscillator versus drain bias at room temperature.

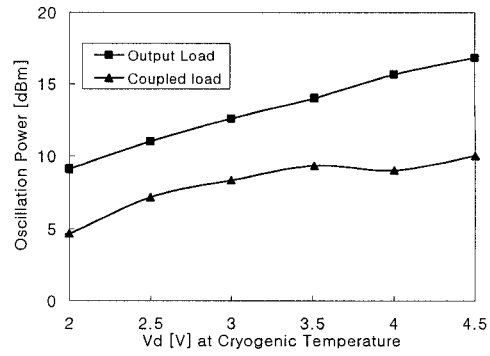

Fig. 8. Load and coupling powers of the implemented HEMT oscillator versus drain bias at cryogenic(4.2K) temperature.

V. Conclusion

We propose new configurations of oscillators with a direct coupling load, and the values of embedding elements are calculated in analytic forms. A X-band HEMT oscillator for Josephson voltage standard is designed and experimented at cryogenic temperature of liquid helium. It is considered that the proposed configurations are useful to reduce the circuit size of oscillator with a coupling load.

References

[1] E. Vollmer, P. G. Gutmann, and Jurgen Niemeyer, "Hybrid integration of a microwave oscillator with a Josephson series array," IEEE Trans. Instrum. Meas., vol. 42, pp 600-602, 19931

[2] Moon-Que Lee, Sangwook Nam, Youngwoo Kwon, and Kyung-Whan Yeom, "Analytic design of high efficiency harmonic loading oscillator using harmonic two signal method", 1997 IEEE MTT-S Digest, Vol. 3, pp. 14951-498

[3] Kenneth M. Johnson, "Large Signal GaAs MESFET Oscillator Design,", IEEE Trans. MTT-27, Mar., 1979, pp217-227

[4] Rowan J. Gilmore, "An Analytic Approach to Optimum Oscillator Design Using S-Parameters," IEEE Trans. MTT-31, Aug., 1983, pp633-639

[5] K.L. Kotzebue, "A Technique for the Design of Microwave Transistor Oscillators," IEEE Trans. MTT-32, July, 1984, pp791-721

[6] O. Llopis, R. Plana, H. Amine, L. Escotte, and J. Graffeuil, "Phase noise in cryogenic microwave HEMT and MESFET oscillator," IEEE Trans. Microwave Theory and Tech. vol. 41, no. 3, march, 1993, pp369-374

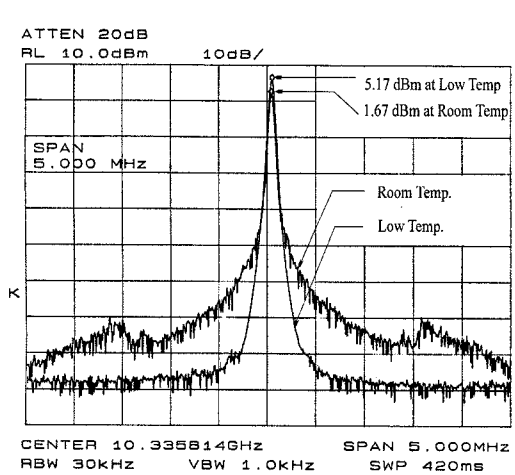

Fig. 9. Comparison between the spectrums of the implemented HEMT oscillator at room and cryogenic temperatures. HEMT is biased at ($V_{gs}=-0.5V$, $V_{ds}=3V$)

Table 1. Values of embedding elements and oscillation range for the series feedback oscillator with a coupling load.

case	external elements	oscillation range
(a)	$\begin{bmatrix} Z_g \\ Z_d \end{bmatrix} = \begin{bmatrix} z_1 & \beta_f \\ z_2 & \beta_b \end{bmatrix} \begin{bmatrix} 1 \\ X_s \end{bmatrix}$	$\mathrm{Re}\{z_1\}-\mathrm{Im}\{\beta_f\}x_s \geq 0$, & $\mathrm{Re}\{z_2\}-\mathrm{Im}\{\beta_b\}x_s \geq 0$
(b)	$\begin{bmatrix} Z_g \\ Z_s \end{bmatrix} = \frac{1}{\beta_b} \begin{bmatrix} \Delta_z & \beta_f \\ -z_2 & 1 \end{bmatrix} \begin{bmatrix} 1 \\ X_d \end{bmatrix}$	$\mathrm{Re}\{\Delta_z\beta_b^*\}-\mathrm{Im}\{\beta_f\beta_b^*\}x_d \geq 0$, & $\mathrm{Re}\{-z_2\beta_b^*\}-\mathrm{Im}\{\beta_b^*\}x_d \geq 0$
(c)	$\begin{bmatrix} Z_s \\ Z_d \end{bmatrix} = \frac{1}{\beta_f} \begin{bmatrix} -z_1 & 1 \\ -\Delta_z & \beta_b \end{bmatrix} \begin{bmatrix} 1 \\ X_g \end{bmatrix}$	$\mathrm{Re}\{-z_1\beta_f^*\}-\mathrm{Im}\{\beta_f^*\}x_s \geq 0$, & $\mathrm{Re}\{-\Delta_z\beta_f^*\}-\mathrm{Im}\{\beta_b\beta_f^*\}x_s \geq 0$
	$z_1=\frac{V_1}{I_1}$, $z_2=\frac{V_2}{I_2}$ $\beta_b=-(1+\frac{I_1}{I_2})=-(1+1/A_I)$, $\beta_f=-(1+\frac{I_2}{I_1})=-(1+A_I)$ $\Delta_z=z_1\times\beta_b-z_2\times\beta_f$	

Table 2. Values of embedding elements and oscillation range for the parallel feedback oscillator with a coupling load.

case	external elements	oscillation range
(d)	$\begin{bmatrix} Y_{gs} \\ Y_{ds} \end{bmatrix} = \begin{bmatrix} y_1 & \alpha_f \\ y_2 & \alpha_b \end{bmatrix} \begin{bmatrix} 1 \\ B_{dg} \end{bmatrix}$	$\mathrm{Re}\{y_1\}-\mathrm{Im}\{\alpha_f\}b_{dg} \geq 0$, & $\mathrm{Re}\{y_2\}-\mathrm{Im}\{\alpha_b\}b_{dg} \geq 0$
(e)	$\begin{bmatrix} Y_{gs} \\ Y_{dg} \end{bmatrix} = \frac{1}{\alpha_b} \begin{bmatrix} \Delta_y & \alpha_f \\ -y_2 & 1 \end{bmatrix} \begin{bmatrix} 1 \\ B_{ds} \end{bmatrix}$	$\mathrm{Re}\{\Delta_y\alpha_b^*\}-\mathrm{Im}\{\alpha_f\alpha_b^*\}b_{ds} \geq 0$, & $\mathrm{Re}\{-y_2\alpha_b^*\}-\mathrm{Im}\{\alpha_b^*\}x_{ds} \geq 0$
(f)	$\begin{bmatrix} Y_{dg} \\ Y_{ds} \end{bmatrix} = \frac{1}{\alpha_f} \begin{bmatrix} -y_1 & 1 \\ -\Delta_y & \alpha_b \end{bmatrix} \begin{bmatrix} 1 \\ B_{gs} \end{bmatrix}$	$\mathrm{Re}\{-y_1\alpha_f^*\}-\mathrm{Im}\{\alpha_f^*\}b_{gs} \geq 0$, & $\mathrm{Re}\{-\Delta_y\alpha_f^*\}-\mathrm{Im}\{\alpha_b\alpha_f^*\}b_{gs} \geq 0$
	$y_1=\frac{I_1}{V_1}$, $y_2=\frac{I_2}{V_2}$ $\alpha_f=-1+\frac{V_2}{V_1}=-1+A_V$, $\alpha_b=-1+\frac{V_1}{V_2}=-1+1/A_V$ $\Delta_y=y_1\times\alpha_b-y_2\times\alpha_f$	